Bima Journal of Science and Technology Vol. 2 No. 1 January, 2018 ISSN25366041

PREPARATION AND CHARACTERIZATIONS OF HYDROXYAPATITE-SODIUM ALGINATE NANOCOMPOSITES FOR BIOMEDICAL APPLICATIONS

F.G Okibe[1], C.C Onoyima[2]
Department of Chemistry, Ahmadu Bello University Zaria, Nigeria
Department of Chemistry, Nigerian Police Academy Wudil, Nigeria
krissonoss@yahoo.co.uk

Abstract

Polymer-inorganic nanocomposites are presently impacting diverse areas, specifically in biomedical sciences. In this research, hydroxyapatite-sodium alginate has been prepared, and characterized, with emphasis on the influence of sodium alginate on its characteristics. In situ wet chemical precipitation method was used in the preparation. The prepared nanocomposite was characterized with Fourier Transform Infrared spectroscopy (FTIR), Scanning Electron Microscopy (SEM), with image analysis, and X-Ray Diffraction (XRD). The FTIR study shows peaks characteristics of hydroxyapatite and confirmed formation of the nanocomposite via chemical interaction between sodium alginate and hydroxyapatite. Image analysis shows the nanocomposites to be of irregular morphologies which did not show significant change with increasing sodium alginate addition, while particle size decreased with increase in sodium alginate addition (359.46 nm to 109.98 nm).From the XRD data, both the crystallite size and degree of crystallinity also decreased with increasing sodium alginate composition (32.36 nm to 9.47 nm and 72.87% to 1.82% respectively), while the specific surface area and microstrain increased with increasing sodium alginate composition (0.0041 to 0.0139 and 58.99 m^2/g to 201.58 m^2/g respectively). The results show that the formulation with 50%wt of sodium alginate (HASA-50%wt), possess exceptional characteristics for biomedical applications such as drug delivery.

Keywords: Nanocomposite, sodium alginate, hydroxyapatite, biomedical, FTIR, XRD, SEM

Introduction

Sodium alginate is a naturally occurring, water soluble linear polysaccharide polymer extracted from brown sea weed and is composed of alternating blocks of 1-4 linked α-L-guluronic acid and β-D-mannuronic acid residues (Kato *et al*., 2003). Due to its many unique properties such as biocompatibility, biodegradability, low toxicity, non-immunogenicity, water solubility, relatively low cost, gelling ability, stabilizing properties (Aggarwal *et al*., 2012), sodium alginate has been widely used in biomedical and pharmaceutical field, including many controlled drug and protein delivery applications (Wells and Sheardown 2009; Chan and Neufeld, 2010; Lee and Lee, 2009); wound dressing (Balakrishnan *et al*., 2006; Murakami *et al*., 2010); cell culture (Wang et al., 2003; Bidarra et al., 2010) tissue engineering and cell delivery

(Skaugrud *et al* 1999; Silva *et al*., 2008; Thornton *et al*., 2004).

On the other hand, there is also growing interest in the use of hydroxyapatite as biomaterial such as drug delivery, orthopedic and dental applications (Mateus *et al*., 2008). However, recent researches have shown that the use of nanocomposite can give rise to materials with novel properties that cannot be obtained by single material. In polymer-inorganic nanocomposite, the inorganic minerals such as hydroxyapatite, silica, metal oxides or calcium phosphate are incorporated into polymer matrices, to impact bioactivity, leading to composites with desired properties (Rajkumar *et al*., 2010). The novel property of the nanocomposite is as a result of physical or covalent interaction with the polymer chain (Goenka *et al.*, 2014).

Hydroxyapatite/polymer composites have attracted much attention since such composite lead to improved properties (Khaled *et al*., 2014) as a result of improvement in the surface functionality of the apatite (Venkatesan *et al.*, 2011). Such improvement has led to wide applications of hydroxyapatite polymer composite in many areas such as in drug delivery system (Andronescu *et al*., 2010;Venkatesan *et al*., 2011; Sivakumar, and Rao, 2012; Raj *et al*., 2013), cell culture and tissue engineering (Haraguchi, 2012; Stodolak-Zycha *et al*., 2012; Zo *et al*., 2012), dental technology (Lee *et al*., 2016), antimicrobials (Castro-Mayorga *et al.*, 2016), energy storage applications (Yang *et al*., 2015; Liu *et al*., 2016), pollution remediation (Ganigar *et al*., 2010; Soni*et al*., 2012; Gardi *et al*., 2015), and so on.

The aim of this research is to prepare hydroxyapatite-sodium alginate and to study the effect of sodium alginate on the prepared composite for potential biomaterial applications.

Methodology

Preparation of Hydroxyapatite/Sodium Alginate Nanocomposites

Preparation of hydroxyapatite-sodium alginate nanocomposite was done according a method reported by Rajkumar *et al*., (2010). This involves an in situ wet chemical precipitation method whereby the hydroxyapatite was precipitated in the presence of sodium alginate. The precursors chosen for the hydroxyapatite were calcium nitrate tetrahydrate ($Ca(NO_3)_2.4H_2O$) (0.1M) and disodium hydrogen phosphate ($(NH_4)_2HPO_4$) (0.06M) for Calcium and Phosphorus sources respectively. The moles were chosen in such a way as to give Ca/P molar ratio of 1.67 which is the stoichiometric amount in pure hydroxyapatite; the calcium nitrate solution was added in dropwise manner to a sodium alginate solution (1%wt) with vigorous stirring. The mixture was then added drop by drop to the hydrogen phosphate solution with continuous stirring, which was continued for 24 hours. The pH was maintained at approximately 10.5 throughout the experiment using sodium hydroxide (hydroxyapatite is precipitated at alkaline pH; and pH of less than 9 can lead to formation of calcium deficient hydroxyapatite). It was allowed

to stand for another 24 hours at room temperature, after which the precipitate was separated by centrifugation and subsequently washed with distilled water three times. The precipitate was dried at 60 ^{0}C for 12 hours and then ground to obtain fine powders.

The same procedure was repeated using varying quantities of sodium alginate (5%wt, 20%wt, 33%wt, and 50%wt). Similarly, the pure nano-hydroxyapatite was prepared using the above method without sodium alginate.

Fourier-Transform Infrared Spectroscopy (FTIR)

FT-IR analysis was conducted to identify the functional groups of the samples. Infrared spectra in the wavenumber range of 650-4000 cm^{-1} were recorded with Cary 630 Agilent Fourier Transform infrared spectrometer. The analyses were carried out with 8 scans at 16 cm^{-1} resolution, applying transmittance method.

Scanning Electron Microscopy (SEM)

The hydroxyapatite and the composites containing different concentrations of sodium alginate were characterized using Scanning Electron Microscope (SEM). The powdered samples were placed on standard aluminum specimen mounts (pin type) with double-sided adhesive electrically conductive carbon tape. The specimen mounts were then coated with 60% Gold and 40% Palladium for 30 seconds with 45 mA current in a sputter coater. The coated samples were then observed on the SEM using an accelerating voltage of 20 kV at a tilt angle of 30^0.

Image Analysis

Image analysis of the particles was carried out using ImageJ software. ImageJ measures directly the projected areas of the particles, the Feret diameter, and the aspect ratio among others, while the spherical equivalent diameter and the aspect ratio were estimated from equation 1 and 2 respectively. An image analysis system could describe non-spherical particles using the Feret diameter, perimeter, projected area, spherical equivalent diameter, circularity and aspect ratio (*ISO 9276-6: (2008*):

Spherical equivalent diameter (SED), = $\sqrt{\frac{4A}{\pi}}$ (1)

This is the diameter of a circle with the same area as the particle. Where, A is the area of the particle.

Aspect ratio (A.R)=$\frac{\text{minor axis}}{\text{major axis}}$ (2)

X-Ray Powder Diffraction Analysis

The X-ray powder diffraction (XRD) patterns were measured on X-ray diffractometer Rigaku Ultima IV (reflection mode, Brag-Brentano arrangement, CuKα1 radiation) in ambient atmosphere under constant conditions (40 kV, 40 mA). The scanning range was 10^0 – 70^0, with scanning step of 0.02.

The crystallite size was calculated using Scherrer equation given below:

$D=\frac{0.89\lambda}{\beta cos\theta}$ (3)

Where D is the average crystallite size, λ is the wavelength of the incident radiation, β is the corrected full width at half

maximum (FWHM) (corrected for instrumental broadening), θ is the diffraction angle. The strongest diffraction peak was used to calculate the crystallite size. Microstrain was estimated using the Williamson-Hall method:

$$B\cos\theta = -\frac{K\lambda}{D} + \varepsilon\sin\theta \quad (4)$$

Where, ε is the strain.

The degree of crystallinity (X_c) was calculated using the equation:

$$X_c = \left(\frac{0.24}{\beta}\right)^3 \quad (5)$$

The specific surface area (S) was calculated with the equation below:

$$S = \frac{6\,x10^3}{Dx\rho} \quad (6)$$

Where ρ is the theoretical density

Results and discussion

FTIR Study

The FTIR spectra of Hydroxyapatite (HA), Sodium alginate (SA), and hydroxyapatite-sodium alginate nanocomposites are shown in Figure 1. The observed functional groups present in hydroxyapatite and their corresponding assignments are illustrated in Table 1. The result confirmed the presence of hydroxyapatite and corresponded well with literature values (Sakthivel and Ragu, 2015; Nabipour et al., 2016; Mehta et al., 2016).

The spectrum of HASA in Figure 1 confirmed chemical interaction between the sodium alginate and hydroxyapatite in the formation of the composite. It was observed that the peak at 3236.3 cm^{-1} due to O-H stretching vibration in sodium alginate shifted to 3220.4 cm^{-1}, while the peak at 1595.3 cm^{-1} and 1405.2 cm^{-1} due to COO^- stretching mode shifted to 1599.0 cm^{-1} and 1408.9 cm^{-1} respectively. The observed shifts are due to replacement of sodium ions in the sodium alginate, which changed the charge density and radius/atomic weight of the cation, creating a new environment around the carbonyl group (Azami *et al*., 2010). The peak at 1341.8 cm^{-1} also confirmed the formation of chemical bond between carbonyl group and divalent metal (COO-Ca) (Kikuchi et al., 2004; Itoh et al., 2005; Azami*et al*., 2010).

Scanning Electron Micrograph (SEM) and Image Analysis

The SEM micrographs of different formulations of hydroxyapatite-sodium alginate nanocomposites are presented in Figure 2. Image analysis was used to calculate particle size and morphological characterization of hydroxyapatite-sodium alginate nanocomposites (HASA).The results show variation in particle size, both the Feret diameter and the spherical equivalent diameter across the different formulations. The trend is observed by plotting the mean values in Figure 3. Addition of 1%wt of sodium alginate to the Hydroxyapatite led to increase in particle size from 127.38 nm to 359.46 nm, however, on further addition of sodium alginate, the particle size decreased, reaching a minimum value of 109.98 nm at HASA-50%wt**.** Similar observation was made by Cunniffe et al., (2010**)** for the synthesis of hydroxyapatite/poly (vinyl alcohol). Cunniffe *et al*., (2010**)** explained that the initial increase in particle size is due to agglomeration/crystallization of

hydroxyapatite; however, on further addition of the polymer there was inhibition on hydroxyapatite aggregation which leads to decrease in particles size.

On the other hand, there was no significant change in the morphology of the particles with increase in composition of sodium alginate as aspect ratio and circularity remained fairly constant (Figure 3). The wide difference between the spherical equivalent diameter and the Feret diameter is a further evidence of non-spherical morphology of the particles. The more spherical the particles are the closer the values of spherical equivalent diameter and Feret diameter.

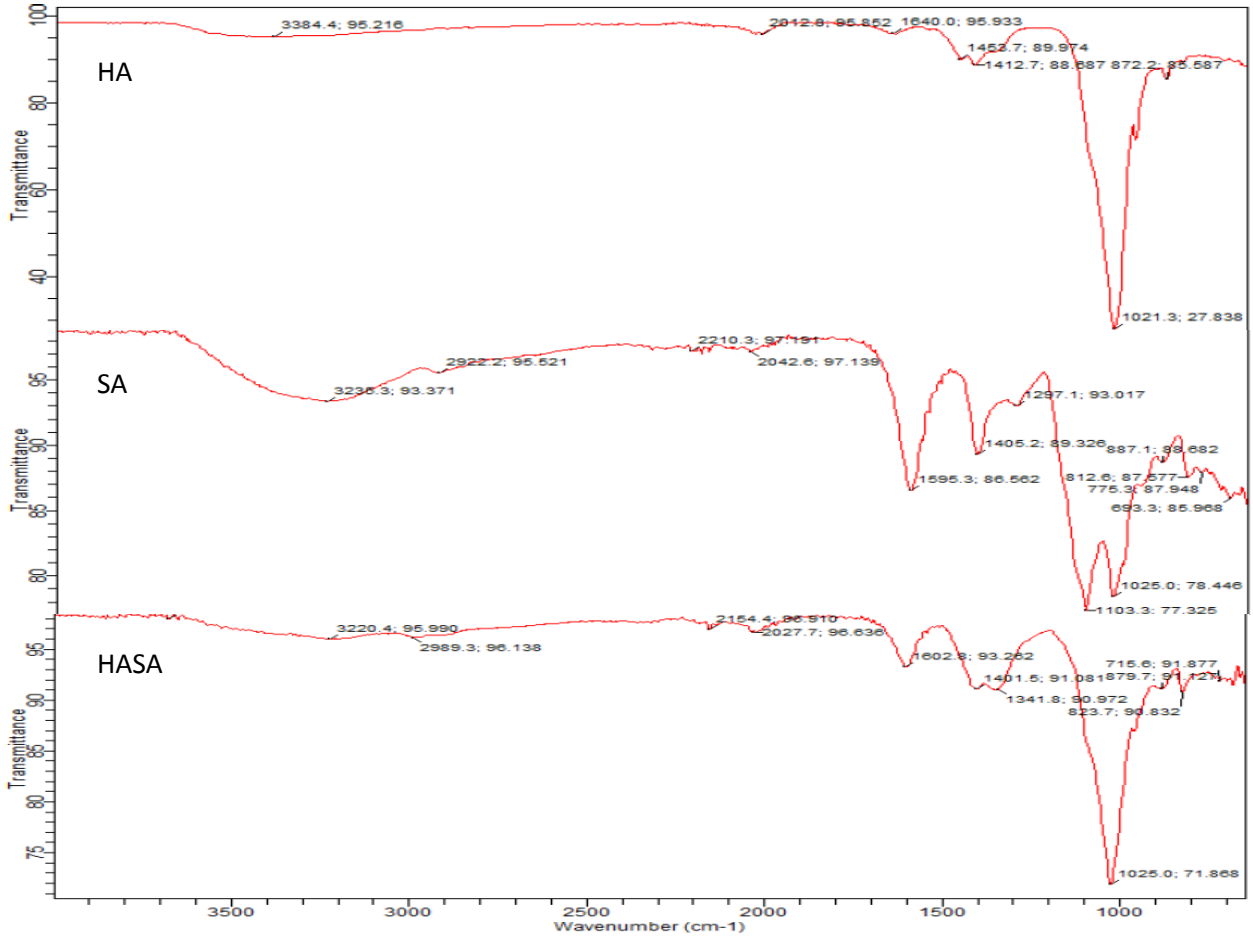

Figure 1: FTIR spectra of hydroxyapatite (HA), Sodium alginate (SA), and Hydroxyapatite- sodium alginate nanocomposite

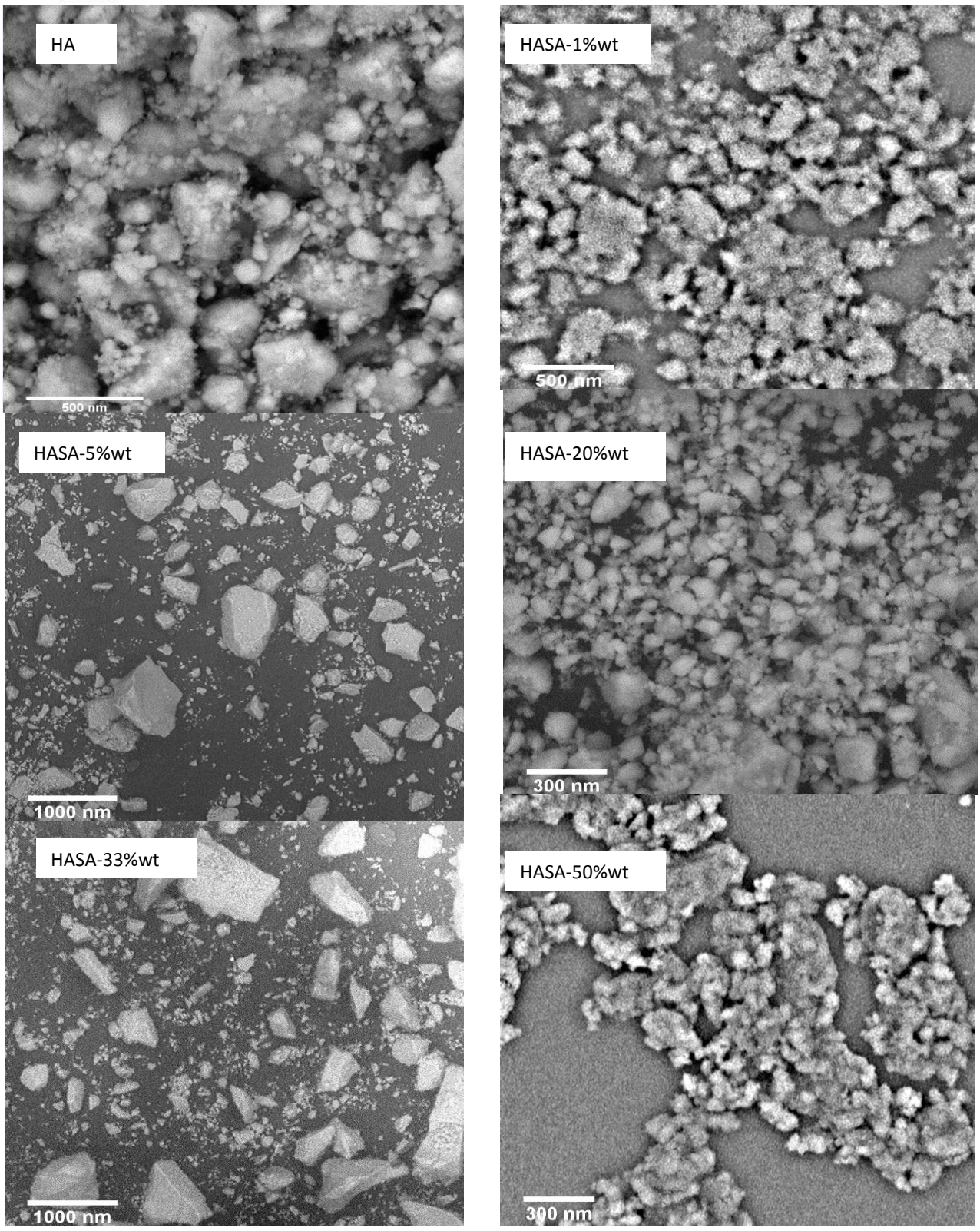

Figure 2: The SEM micrograph of hydroxyapatite-sodium alginate nanocomposites (HASA)

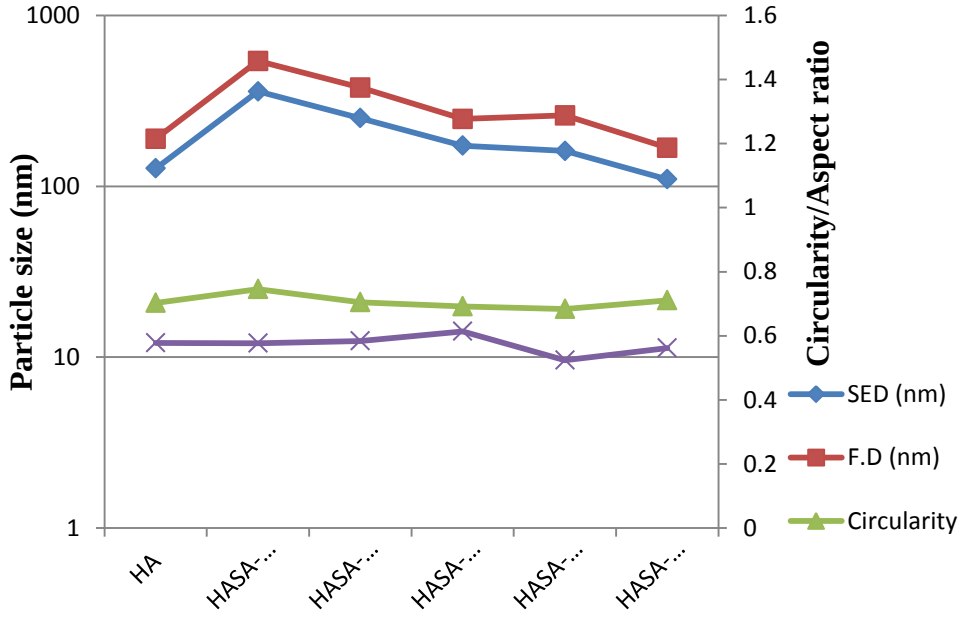

Figure 3: Variation of size and morphology of the particles with increase in composition of Sodium alginate

The XRD spectra shown in Figure 4 identified the major peaks at 2θ = 25.88^0 (d-value = 3.4394 Å), 31.77^0 (d-value = 2.8144 Å), and 32.15^0 (d-value = 2.7818 Å), which were assigned Miller indices of (002), (121), and (112) planes respectively. These planes were present in all the hydroxyapatite-sodium alginate samples. There was no notable effect on the peak positions with the addition of sodium alginates. However, there was significant broadening which can be due to a combination of size and strain effect. This was further evaluated using the full width at half maximum values (FWHM) and applying appropriate equations for size and strain.

The crystallite sizes of both HA and HASA were calculated using the Scherrer formula (Equation3) for (121) planes, which is the strongest peak. Scherrer formula assumes that the strain contribution to the peak broadening is negligible. The results reveal that the crystallite size decreases with increase in the composition of sodium alginate (Figure 5). The values range from 9.47 nm to 32.36 nm. Decrease in the crystallite size of HA with addition of polymer has been reported for HA/PVA **(**Rajkumar *et al*., 2010**)**, HA/PVA **(**Cunniffe *et al*., 2010**).**

There was also significant reduction in particles yield as particles size decreases. The smaller the particle size, the more difficult it is to recover the particles from solution.

Like crystallite size, the degree of crystallinity also decreased with increase in composition of sodium alginate. From equation 3 and 5, both crystallite size and degree of crystallinity varies inversely as the full width at half maximum value (FWHM). As the crystals become smaller, the contribution to the peak broadening increases (i.e. increase in the value of FWHM), and consequently the degree of crystallinity increases. According to Kucherov

et al., (2003) materials with low crystallinity are preferred for biomaterial purposes due to their high in-vivo resorbability.

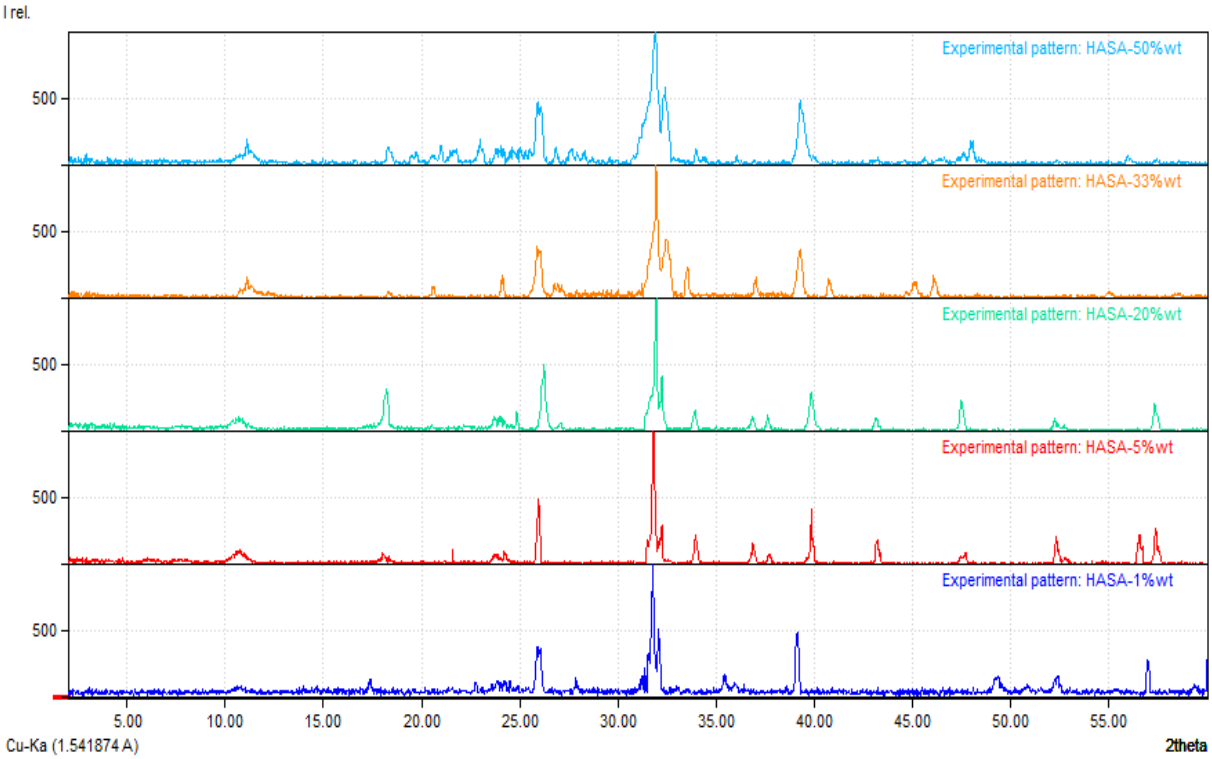

Figure 4: XRD Spectra of Different Formulations of Hydroxyapatite-Sodium Alginate nanocomposites

Table 1: Assignments of FTIR peaks of hydroxyapatite

Wave number	Assignments
3384.4	O-H stretching vibration
2012	overtone and/or combinational bands of PO_4^{3-} groups
1640	O-H bending mode of absorbed water
1453.7	CO_3^{2-} asymmetric stretching
1412.7	CO_3^{2-} asymmetric stretching
1021.3	asymmetric stretching of PO_4^{3-}
960	PO_4^{3-} symmetric stretching
872.2	CO_3^{2-}symmetric stretching

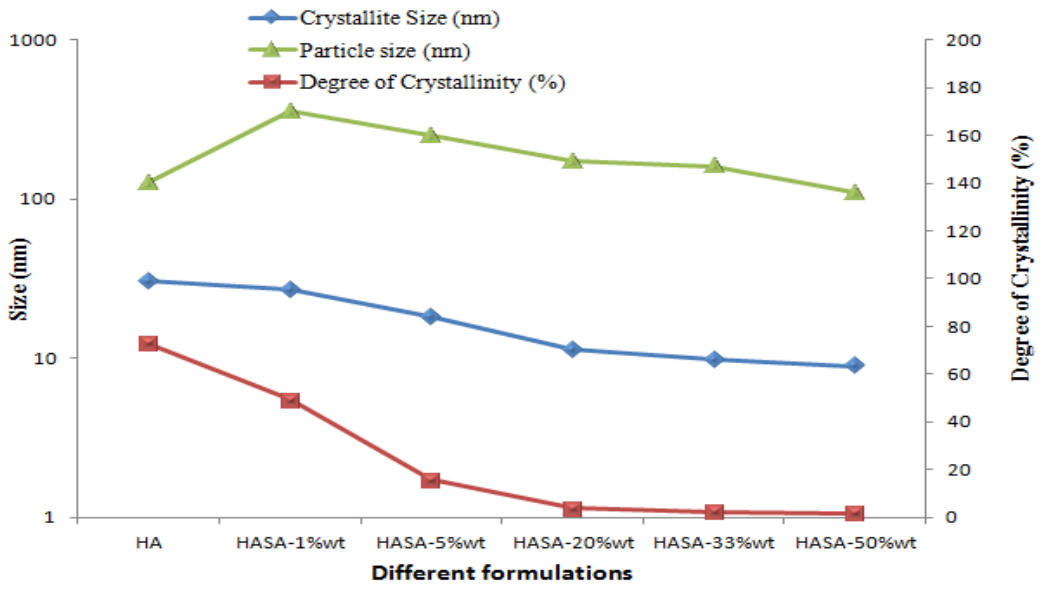

Figure 5: Effects of quantity of sodium alginate on the particle size, crystallite size and degree of crystallinity of Hydroxyapatite

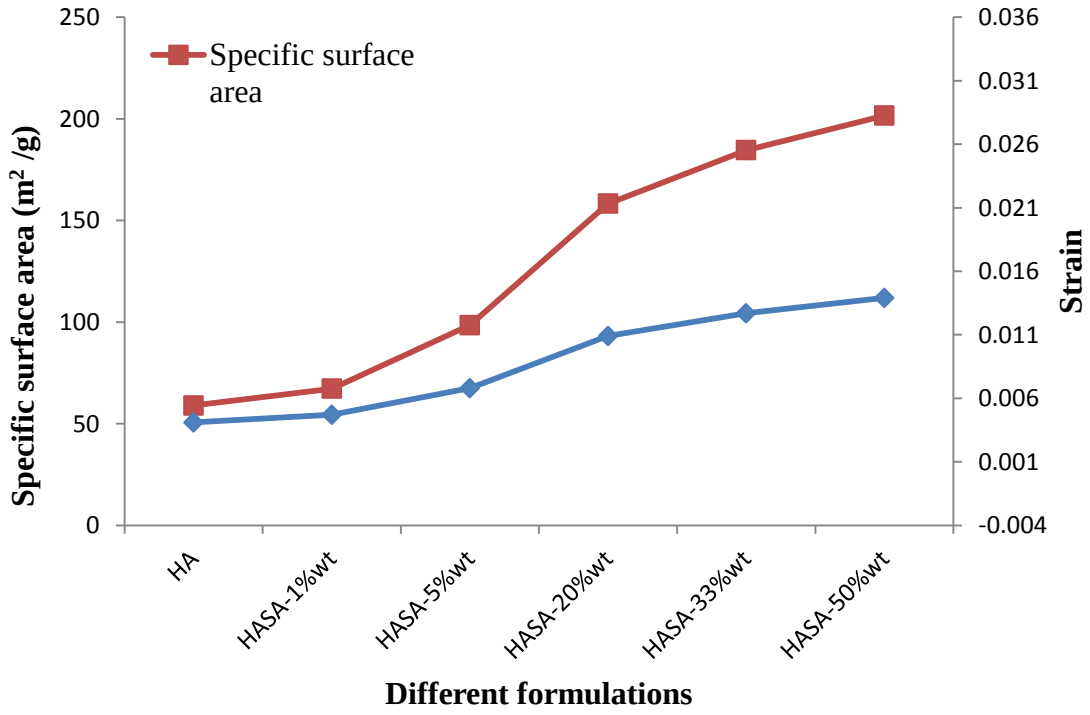

Figure 6: Variation of microstrain and specific surface area with the quantity of sodium alginate

Conclusion

Hydroxyapatite-sodium alginate has been prepared. The properties of the prepared nanocomposite depended on the quantity of sodium alginate incorporated. The prepared nanocomposites are of nanometre size range. It was shown that particle size and crystallite size decreased while strain and specific surface area increased with increasing sodium alginate composition. The formulation with 50% wt of sodium alginate (HASA-50%wt), possesses better satisfactory characteristics than other formulations for biomedical applications such as drug delivery applications.

References

Aggarwal S; Goel A and Singla S. (2012). Drug delivery: special emphasis given on biodegradable polymers. *Advances in Polymer Science and Technology: An International Journal*, 2 (1), 1-15.

Andronescu, E., Ficai, M., Voicu, G., Ficai, D., Maganu, M and Ficai, A. (2010). Synthesis and characterization of collagen/hydroxyapatite: magnetite composite material for bone cancer treatment. *Journal of Materials Science: Materials in Medicine*, 21(7), 2237-2242. doi:101007/s10856-010-4076-7

Azami, M., Samadikuchaksaraei, A and Poursamar, S.A. (2010).Synthesis and characterization of a laminated hydroxyapatite/gelatin nanocomposite scaffold with controlled pore structure for bone tissue engineering. *International Journal of Artificial Organ*, 33 (2): 86-95.

Baig, A.A., Fox, J.L., Young, R.A., Wang, Z., Hsu, J., Higuchi, W.I, Chnetty, A., Zhang, H., and Otsuka, M. (1999).Relationship among carbonated apatite solubility, crystallite size, and microstain parameters.*Calif Tissue Internationals*, 64(5), 437 – 490.

Balakrishnan B, Mohanty M, Fernandez A.C, Mohanan P.V, Jayakrishnan A. (2006). Evaluation of the effect of incorporation of dibutyryl cyclic adenosine monophosphate in an in situ forming hydrogel wound dressing based on oxidized alginate and gelatin. *Biomaterials*, 27, 1355–1361.

Balakrishnan, B., Mohanty, M., Fernandez, A.C., Mohanan, P.V., Jayakrishnan, A. (2006). Evaluation of the effect of incorporation of dibutyryl cyclic adenosine monophosphate in an in situ forming hydrogel wound dressing based on oxidized alginate and gelatin. *Biomaterials*, 27, 1355–1361.

Bidarra, S.J., Barrias, C.C., Barbosa, M.A., Soares, R., Granja, P.L. (2010). Immobilization of human mesenchymal stem cells within RGD-grafted alginate microspheres and assessment of their angiogenic potential.*Biomacromolecules*, 11, 1956–1964.

Castro-Mayorga, J.L.,Fabra,M.J and Lagaron, J.M. (2016). Synthesis, characterization and antimicrobial properties of zinc oxide

nanoparticles and poly(3-hydroxybutyrate-co-3-hydroxyvalerate) films produced by electrospinning 6th International Seminar on Modern Polymeric Materials for Environmental Applications, 27-29 April, 2016, Kraków, Poland.

Chan A.W, and Neufeld R.J. (2010). Tuneable semi-synthetic network alginate for absorptive encapsulation and controlled release of protein therapeutics.*Biomaterials*, 31, 9040–9047.

Cunniffe, G.M., O'Brien, F.J., Partap, S., Levingstone, T.J., Stanton, K.T and Dickson, G.R. (2010). The synthesis and characterization of nanophase hydroxyapatite using a novel disperant-aided precipitation method. *Journal of Biomedical Materials Research. Part A*, 95(4):1142-9.

Ganigar, R., Rytwo, G., Gonen, Y., Radian, A and Mishael, Y.G. (2010). Polymer-clay nanocomposites for the removal of trichlorophenol and trinitrophenol from water.*Applied Clay Science*, 49: 311-316.

Gardi, I., Nir, S andMishael, Y.G. (2015). Filtration of triazine herbicides by polymer-clay sorbents: Coupling an experimental mechanistic approach with empirical modeling. *Water Research* 70: 64-73.

Goenka, S., Sant, V and Sant, S. (2014). Graphene-based nanomaterials for drug delivery and tissue engineering. *Journal of Control Release*, 173(1), 75–88.

Haraguchi, K. (2012). Development of Soft Nanocomposite Materials and Their Applications in Cell Culture and Tissue Engineering. Journal of Stem Cell and Regenerative Medicine, 8(1): 2-11.

ISO, *ISO 9276-6: (2008*). Representation of results of particle size analysis– Part 6: Descriptive and quantitative representation of particle shape and morphology.

Itoh, S., Kikuchi, M and Koyama, Y. (2005). Development of a novel biomaterial, ydroxyapatite/collagen (HAp/Col) composite for medical use. *Biomedical and Material Engineering*, 15, 29-41.

Kato, Y., Onishi, H., & Machida, Y. (2003). Application of chitin and chitosan derivatives in the pharmaceutical field. *Current Pharmaceutical Biotechnology*, 4, 303–309.

Khaled R. M; Hanan H. B, and Zenab M. E. (2014).In-vitro study of nano-hyroxyapatite/gelatine-chitosan composites for bio-application. *Journal of Advanced Research*, 5, 201 – 208.

Kikuchi, M., Matsumoto, H.N., Yamada, T., Koyama, Y., Takakuda, K and Tanaka, J. (2004). Glutaraldehyde cross-linked hydroxyapatite/collagen self-organized nanocomposites. *Biomaterials*, 25, 63-69.

Kucherov, A.V., Kramareva, N.V., Finashina, E.D., AKoklin, A.E andKustov, L.M. (2003).

Heterogenized redox catalysts on the basis of the chitosan matrix Copper complexes *Journal of Molecular Catalalysis A*, 198, 377–89.

Lee, J., and Lee, K.Y. (2009). Injectable microsphere/hydrogel combination systems for localized protein delivery. *Macromolecules and Bioscience*, 9, 671–676.

Lee,J., Kim, H and Seo, S.. (2016). Polymer-Ceramic Bionanocomposites for Dental Application. *Journal of Nanomaterials*, 2016, 1-8.http://dx.doi.org/10.1155/2016/3795976.

Liu, S., Xiu, S., Shen, B., Zhai, J and Bing Kong, L.B. (2016). Dielectric Properties and Energy Storage Densities of Poly(vinylidenefluoride) Nanocomposite with Surface Hydroxylated Cube ShapedBa0.6Sr0.4TiO3 Nanoparticles. *Polymers*, 8, 45 doi:10.3390/polym8020045

Mateus, A.Y.,Barrias, C.C.,Ribeiro, C., Ferraz, M. P and Monteiro, F. J. (2008). Comparative study of nanohydroxyapatite microspheres for medical applications. *Journal of Biomed Material Resource A* 86, 483 – 93.

Mehta, D., George, S and Singh, A. (2016). Assessment of Different Synthesis Route of Hydroxyapatite and Study of its Biocompatibility in Synthetic Body Fluids. International Journal of ChemTech Research, 9(3): 267-276.

Murakami K, Aoki H, Nakamura S, Nakamura S, Takikawa M, Hanzawa M, Kishimoto S, Hattori H, Tanaka Y, Kiyosawa T, Sato Y, Ishihara M. (2010). Hydrogel blends of chitin/chitosan, fucoidan and alginate as healing-impaired wound dressings. *Biomaterials*, 31, 83–90.

Murakami, K., Aoki, H., Nakamura, S., Nakamura, S., Takikawa, M., Hanzawa, M., Kishimoto, S, Hattori H, Tanaka Y, Kiyosawa T, Sato Y and Ishihara M. (2010). Hydrogel blends of chitin/chitosan, fucoidan and alginate as healing-impaired wound dressings. *Biomaterials*, 31, 83–90.

Nabipour, Z, Nourbakhsh, M.S and Baniasadi, M. (2016). Synthesis, characterization and biocompatibility evaluation of hydroxyapatite -gelatin polyLactic acid ternary nanocomposite.Nanomedicine Journal, 3(2): 127-134. **DOI:** 10.7508/nmj.2016.02.006.

Raj M.S,Arkin V.H, Adalarasu and Jagannath M. (2013). Nanocomposites Based on Polymer and Hydroxyapatite for Drug Delivery Application. *Indian Journal of Science and Technology*, 6(5S), 4653 – 4658.

Rajkumar M, Sundaram N.M and Rajendran V. (2010). In-situ preparation of hydroxyapatite nanorod embedded poly (vinyl alcohol) composite and its characterization. *International Journal of Engineering Science*

and Technology, 2(6), 2437 – 2444.

Sakthivel, P and Ragu, A. (2015). Synthesis and Characterization of Nano Hydroxyapatite with Polymer Matrix Nano Composite for Biomedical Applications International Journal of Chemical, Environmental & Biological Sciences (IJCEBS), 3(5): 383-385.

Silva E.A, Kim E.S, Kong H.J and Mooney D.J. (2008). Material-based deployment enhances efficacy of endothelial progenitor cells. ProcNatlAcadSci USA, 105, 14347–14352.

Sivakumar M, and Rao K.P. (2002). Preparation, characterization and in vitro release of gentamicin from coralline hydroxyapatite–gelatin composite microspheres. *Biomaterials*, 23, 3175 – 3181.

Skaugrud O, Hagen A, Borgersen B, and Dornish M. (1999). Biomedical and Pharmaceutical application of alginate and chitosan. *Biotechnology and Genetic Engineering Review*, 16, 23 – 40.

Skaugrud, O., Hagen, A., Borgersen, B., and Dornish, M. (1999). Biomedical and Pharmaceutical application of alginate and chitosan. *Biotechnology and Genetic Engineering Review*, 16, 23 – 40.

Soni, A., Tiwari, A and Bajpal, A.K. (2012). Adsorption of o-nitrophenol onto nano iron oxide and alginate microspheres: Batch and column studies. *African Journal of Pure and Applied Chemistry* 6: 161-173.

Stodolak-Zycha, E., Fraczek-Szczyptaa, Wiechecb, A and Błazewicz, M. (2012). Nanocomposite Polymer Scaffolds for Bone Tissue Regeneration.*Acta Physica Polonica A*, 121(2), 518-521.

Thornton A.J, Alsberg E, Albertelli M, Mooney D.J. (2004). Shape-defining scaffolds for minimally invasive tissue engineering. *Transplantation*, 77, 1798–1803.

Venkatesan P, Puvvada N, Dash R, Kumar B.N, Devanand S, Azab B, Pathak A, Kundu S.C, Fisher P.B and Mandal M. (2011). The potential of celecoxib-loaded hydroxyapatite-chitosan nanocomposite for the treatment of colon cancer. *Biomaterial*, 32, 3794 – 3806.

Venkatesan P, Puvvada N, Dash R, Kumar B.N, Devanand S, Azab B, Pathak A, Kundu S.C, Fisher P.B and Mandal M. (2011). The potential of celecoxib-loaded hydroxyapatite-chitosan nanocomposite for the treatment of colon cancer. *Biomaterial*, 32, 3794 – 3806.

Wang L, Shelton R.M, Cooper P.R, Lawson M, Triffitt J.T and Barralet J.E. (2003). Evaluation of sodium alginate for bone marrow cell tissue engineering. *Biomaterials*, 24, 3475–3481.

Wang, L., Shelton, R.M., Cooper, P.R., Lawson, M., Triffitt, J.T and Barralet, J.E. (2003). Evaluation of sodium alginate for bone marrow cell tissue engineering. *Biomaterials*, 24, 3475–3481.

Wells LA, and Sheardown H. (2009). Extended release of high pI proteins

from alginate microspheres via a novel encapsulation technique. *Europian Journal of Pharmacy and Bio pharmacy*, 65, 329–335.

Yang, C., Wei, H.,Guan, L.,Guo,J.,Wang, Y., Yan, X., Zhang, X., Suying Wei, Sand Guo, Z. (2015). Polymer nanocomposites for energy storage, energy saving, and anticorrosion. *Journal of Materials Chemistry A*, 3, 14929-14941.DOI: 10.1039/c5ta02707a

Zo, S.M., Singh, D., Kumar, A., Cho,Y.W., Oh, T.H and Han, S.S. (2012). Chitosan–hydroxyapatite macroporousmatrix for bone tissue engineering. *Current Science*,103(12): 1438-1446.